Data-aided Weight with Subcarrier Grouping for Adaptive Array Interference Suppression

He He, Jun-Han Wang, *Student Member, IEEE,* Shun Kojima, *Member, IEEE,* Kazuki Maruta, and Chang-Jun Ahn, *Senior Member, IEEE*

Original scientific article

***Abstract*—The effect of additive noise on the channel state information (CSI) quality is a crucial issue in mobile communication systems. The adaptive subcarrier grouping (ASG) for sample matrix inversion (SMI) based minimum mean square error (MMSE) adaptive array has been previously proposed. However, this method needs to know the signal-to-noise ratio (SNR) in advance to set the threshold, perform grouping, and take the average, causing an insufficient number of signal samples. As a result, the ability to eliminate noise is limited. In this paper, we propose a new method based on data-aided weight calculation and the least mean square (LMS) algorithm without SNR information, which increases the number of samples. The decision results and initial weight are obtained by the SMI method with subcarrier grouping, and then the LMS method with subcarrier grouping is applied to reduce the channel estimation error as well as the amount of computation. Simulation results demonstrate that the proposed scheme is an efficient approach to improve Bit Error Rate (BER) performance under various Rician K factors.**

***Index Terms*—Noise effect, sample matrix inversion, subcarrier grouping, decision feedback, least mean square.**

I. Introduction

With the advent of Internet-of-Things (IoT), mobile data traffic, as well as the number of movable devices and connections, has been rapidly increasing in cellular networks. Increasing transmission rates and realizing huge system capacity are essential for the fifth generation of mobile communications (5G) and beyond [1], [2]. Therefore, millimeter wave (mmWave) is used as the ideal communication technology to solve the above problems [3]. Millimeter wave communication systems exploit the ultra-high frequency (EHF) band for broadband communications where there is still a large amount of available spectrum for communications [4]. However, it suffers from severe propagation loss, causing restricted coverage and a link budget shortfall. The deployment of a massive MIMO-small cell system [5] is one of the promising solutions to reduce the attenuation of radio waves. By setting the phase shifts of all the antenna elements to obtain beamforming gain, the signal to interference plus noise ratio (SINR) can be can maximized in massive MIMO. Small cells can manage high traffic demand within the coverage area of macrocells [6], [7]. In the small cells, the propagation environment is dominated by a line of sight (LOS) component for a reliable communication system. Therefore, Rician distribution with LOS and non-LOS (NLOS) components is considered as the channel model in this situation [8].

In general, inter-user-interference (IUI) and additive white Gaussian noise are essential for array antenna. Sample matrix inversion(SMI) [9], [10] is a well-known method for interference suppression adaptive array antennas. SMI utilizes a covariance matrix derived from the pilot symbols and the received signals of each antenna element to calculate desirable weights. Due to the inaccurate channel state information (CSI) caused by the additive noise effect, this method requires a sufficient number of samples to adequately suppress interference [11]. In addition, since the array weights are calculated for each subcarrier in orthogonal frequency division multiplexing (OFDM) systems, it causes not only an insufficient number of samples but also a large amount of computation [12]. Further discussion is needed for the OFDM frame. Common Correlation Matrix (CCM) based SMI algorithm has been proposed to reduce the amount of calculation and enhance weight precision for interference suppression performance. In the CCM method, an adequate number of the time domain signal samples can be available for a well-converged covariance matrix [13], [14]. However, it still has a problem of inaccurate channel estimation and the limitation of working only in an almost frequency-flat fading environment since the weight is common in all subcarriers. For this reason, it cannot work in the heterogeneous deployment of small cells. A more recent work evaluates the effect under the above situation [15]. Reference [15] proposed an adaptive subcarrier grouping (ASG) method. In ASG method, the standard deviations among the adjacent subcarriers are calculated, averaged, and compared with the threshold to determine the grouping. It has good performance even in frequency selectivity channels. However, because of an insufficient number of signal samples under the limited number of pilot symbols, there is a problem of insufficient noise suppression performance and the threshold of the grouping must depend on signal-to-noise ratio (SNR). Although there are many methods to estimate SNR [16]- [18], they not only cause the additional computational complexity but the SNR estimation errors, which must be considered in

Manuscript received August 31, 2022; revised October 17, 2022. Date of publication December 13, 2022. Date of current version December 13, 2022.

H. He, J. H. Wang, and C. -J. Ahn are with the Graduate School of Engineering, Chiba University, Chiba-shi, 263-8522 Japan (e-mails: kakukaku@chiba-u.jp, wangjunhan668@gmail.com, junny@faculty.chiba-u.jp).

S. Kojima is with the Graduate School of Engineering, Utsunomiya University, Utsunomiya-shi, 125-8585 Japan (e-mail: s.kojima@ieee.org).

K. Maruta is with the Faculty of Engineering, Tokyo University of Science, Tokyo, 321-8585 Japan (e-mail: kazuki.maruta@ieee.org).

Digital Object Identifier (DOI): 10.24138/jcomss-2022-0109

the ASG method.

This paper proposes to introduce data-aided weight calculation with subcarrier grouping. The proposed method calculates weights by the SMI method with subcarrier grouping and determines the decision result. The benefit of our proposal is that we do not need to know the SNR or other information. This is because the number of subcarriers in each group is the same. In general, more pilot symbols have been used to improve the accuracy of weights. However, an increased number of pilot symbols causes poor transmission efficiency since they do not contribute to data transfer. Another key feature of our proposed method is to expand toward the symbol direction by increasing the amount of sample aided by decision feedback data, which can not only estimate more accurate weight estimation but also maintain transmission efficiency. Moreover, the LMS algorithm with low computational complexity is introduced to ensure convergence while using the initial weights to avoid additional iterations.

The rest of this paper is organized as follows. The system model is defined and conventional schemes are introduced in section II. Section III describes the proposed scheme. Computer simulation results are presented in section IV. Finally, section V concludes this paper.

II. System Model

A. Channel Model

In the Rician fading channel model, there are two components: a deterministic component corresponding to LOS signals and a random component corresponding to NLOS signals [20]. An NLOS multipath fading channel is expressed as,

$$h(\tau)_{\mathrm{NLOS}} = \sum_{l=1}^{L} h_l \delta(t-\tau_l), \tag{1}$$

where δ denotes the Dirac's delta function, τ_l is the time delay of the l-th path and L is the total number of paths. h_l indicates the complex channel coefficient, which is represented as follows known as Jakes' model [21],

$$h_l = \frac{g_l}{\sqrt{J}} \sum_{j=1}^{J} \exp\left(\mathrm{j}\phi_j\right), \tag{2}$$

where g_l denotes the gain of the path. J rays arrive at the receiver with an initial phase ϕ_j. Here assumes the normalized path gain, i.e. $\sum_{l=0}^{L} E\left[\left|h_l^2\right|\right] = 1$ where $E\left[\cdot\right]$ stands for the ensemble average operation. The Rician fading channel is expressed as,

$$h(\tau) = \left[\frac{K}{K+1}\right]^{\frac{1}{2}} h_{\mathrm{LOS}}(\tau) + \frac{h_{\mathrm{NLOS}}(\tau)}{(K+1)^{\frac{1}{2}}}, \tag{3}$$

$$h_{\mathrm{LOS}}(\tau) = h_0 \delta(t-\tau_1), \tag{4}$$

$$h_0 = g_0 \exp\left(\mathrm{j}\phi_0\right), \tag{5}$$

where $h_{\mathrm{LOS}}(\tau)$ represents the LOS fading channel and h_0 is the complex channel coefficient, respectively. Then the frequency response $H(f)$ is obtained by Fourier transform of the impulse response as,

$$H(f) = \sum_{l=0}^{N_{\mathrm{FFT}}-1} h(\tau_l) \exp\left(-\mathrm{j}\frac{2\pi f \tau_l}{N_{\mathrm{FFT}}}\right), \tag{6}$$

where f and N_{FFT} denote the frequency component and the number of fast Fourier transform (FFT) points, respectively.

B. Uplink Array Antenna System Model

We suppose uplink transmission where a base station(BS) has N_{r} elements array antenna and N_{u} user terminals (UEs) with OFDM like Fig.1.

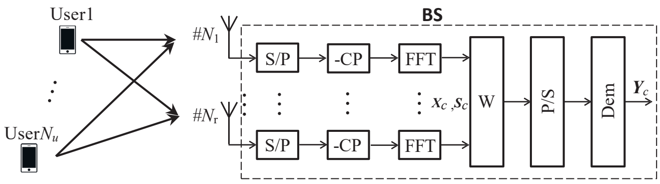

Fig. 1. Block diagram of the basic system.

Throughout this paper, subscripts c and u represent the c-th subcarrier and the u-th user, respectively. Then, the received pilot signal $\boldsymbol{X}_c \in \mathbb{C}^{N_{\mathrm{r}} \times N_{\mathrm{P}}}$, received data signal $\boldsymbol{S}_c \in \mathbb{C}^{N_{\mathrm{r}} \times N_{\mathrm{d}}}$, and array output $\boldsymbol{Y}_c \in \mathbb{C}^{N_{\mathrm{u}} \times N_{\mathrm{d}}}$ can be expressed as follows.

$$\boldsymbol{X}_c = \boldsymbol{A}\boldsymbol{H}_c\boldsymbol{P}_c + \boldsymbol{N}, \tag{7}$$

$$\boldsymbol{S}_c = \boldsymbol{A}\boldsymbol{H}_c\boldsymbol{D}_c + \boldsymbol{Z}, \tag{8}$$

$$\boldsymbol{Y}_c = \boldsymbol{W}_c^{\mathsf{H}}\boldsymbol{S}_c, \tag{9}$$

where

$$\boldsymbol{A} = [\boldsymbol{a}_1, \ldots, \boldsymbol{a}_u, \ldots, \boldsymbol{a}_{N_{\mathrm{u}}}], \tag{10}$$

$$\boldsymbol{H}_c = \mathrm{diag}\left(H_1, \ldots, H_u, \ldots, H_{N_{\mathrm{u}}}\right), \tag{11}$$

$$\boldsymbol{P}_c = [\boldsymbol{p}_1^{\mathsf{T}}, \ldots, \boldsymbol{p}_u^{\mathsf{T}}, \ldots, \boldsymbol{p}_{N_{\mathrm{u}}}^{\mathsf{T}}]^{\mathsf{T}}, \tag{12}$$

$$\boldsymbol{D}_c = [\boldsymbol{d}_1^{\mathsf{T}}, \ldots, \boldsymbol{d}_u^{\mathsf{T}}, \ldots, \boldsymbol{d}_{N_{\mathrm{u}}}^{\mathsf{T}}]^{\mathsf{T}}. \tag{13}$$

$\boldsymbol{A} \in \mathbb{C}^{N_{\mathrm{r}} \times N_{\mathrm{u}}}$, $\boldsymbol{H}_c \in \mathbb{C}^{N_{\mathrm{u}} \times N_{\mathrm{u}}}$, $\boldsymbol{P}_c \in \mathbb{C}^{N_{\mathrm{u}} \times N_{\mathrm{P}}}$, $\boldsymbol{D}_c \in \mathbb{C}^{N_{\mathrm{u}} \times N_{\mathrm{d}}}$, $\boldsymbol{N} \in \mathbb{C}^{N_{\mathrm{r}} \times N_{\mathrm{P}}}$, $\boldsymbol{Z} \in \mathbb{C}^{N_{\mathrm{r}} \times N_{\mathrm{d}}}$,$\boldsymbol{W}_c \in \mathbb{C}^{N_{\mathrm{r}} \times N_{\mathrm{u}}}$ denote array factor matrix, fading channel matrix, transmitted pilot symbols, transmitted data symbol, additive white Gaussian noise (AWGN) matrices of pilot symbols and data symbols, and weight vector, respectively. The array weight vector can cancel interference components.

C. SMI Algorithm

SMI algorithm is based on a minimum mean square error (MMSE) method for solving the minimum searching problem [9], whose weight can be derived as,

$$E[|\boldsymbol{e}|^2] = E[|\boldsymbol{P}_c - \boldsymbol{W}_c^{\mathsf{H}}\boldsymbol{X}_c|^2]. \tag{14}$$

where the pilot symbol $\boldsymbol{P}_c$ is considered as the desired response.

The optimal weight by SMI algorithm is derived as

$$\boldsymbol{\Phi}_c = \boldsymbol{X}_c \boldsymbol{X}_c^{\mathsf{H}}, \tag{15}$$
$$\boldsymbol{V}_c = \boldsymbol{X}_c \boldsymbol{P}_c^{\mathsf{H}}, \tag{16}$$
$$\boldsymbol{W}_c = \boldsymbol{\Phi}_c^{-1} \boldsymbol{V}_c, \tag{17}$$

where $\boldsymbol{\Phi}_c \in \mathbb{C}^{N_\mathrm{r} \times N_\mathrm{r}}$ and $\boldsymbol{V}_c \in \mathbb{C}^{N_\mathrm{r} \times N_\mathrm{u}}$ indicate the covariance matrix and the estimated CSI vector, respectively. However, there is a noise problem in the received signal.

D. Adaptive Subcarrier Grouping (ASG)

In the above scheme, the effect of noise has been not fully considered when calculating the array weight. By exploiting adaptive grouped subcarriers with correlated frequency responses for averaging, the convergence precision of the covariance matrix can be improved [15]. Frist, subcarriers are chosen for grouping to suppress interference. We define m as both the number of stages and the end sequence of a group to delimit a group range from the c-th subcarrier, i.e., the subcarrier sequence corresponding to a group in the m-th stage is $(c, ..., c+m)$. $m = 0$ is initialized as no grouping.

We average the grouped received signal X and pilot signal P from subcarrier c to $c+m$ to reduce noise, which combines the $(m+1)$ subcarriers. The grouped received pilot signal matrix and the grouped transmitted pilot signal matrix for averaging is calculated as follows,

$$\overline{\boldsymbol{X}^{(m)}} = \frac{1}{m+1} \sum_{k=0}^{m} \boldsymbol{X}_{c+k}, \tag{18}$$
$$\overline{\boldsymbol{P}^{(m)}} = \frac{1}{m+1} \sum_{k=0}^{m} \boldsymbol{P}_{c+k}, \tag{19}$$

where $X_{c+k} \in \mathbb{C}^{N_\mathrm{r} \times N_\mathrm{P}}$ and $P_{c+k} \in \mathbb{C}^{N_\mathrm{u} \times N_\mathrm{P}}$ are the $(c+k)$-th subcarrier of the received pilot signal matrix and transmitted pilot signal matrix. $\overline{\boldsymbol{X}^{(m)}} \in \mathbb{C}^{N_\mathrm{r} \times N_\mathrm{P}}$ and $\overline{\boldsymbol{P}^{(m)}} \in \mathbb{C}^{N_\mathrm{u} \times N_\mathrm{P}}$ are the averaged received pilot signal and averaged transmitted pilot signal. Then, a standard deviation of the grouped received sigal, $\boldsymbol{\sigma}_{\mathrm{ASG}}^{(m)} \in \mathbb{C}^{N_\mathrm{r} \times N_\mathrm{P}}$ is calculated as,

$$\boldsymbol{\sigma}_{\mathrm{ASG}}^{(m)} = \sqrt{\frac{1}{m+1} \sum_{k=0}^{m} \left\{ \boldsymbol{X}_{c+k} - \overline{\boldsymbol{X}^{(m)}} \right\}^2}, \tag{20}$$
$$\overline{\sigma_{\mathrm{ASG}}^{(m)}} = \sum_{j=1}^{N_\mathrm{P}} \sum_{i=1}^{N_\mathrm{r}} \sigma_{\mathrm{ASG},i,j}^{(m)} / N_\mathrm{P} N_\mathrm{r}. \tag{21}$$

$\overline{\sigma_{\mathrm{ASG}}^{(m)}}$ represents the dispersion among the grouped subcarriers. Therefore, only frequency-correlated subcarriers are combined by comparing with a threshold value, $\sigma_{\mathrm{ASG}}^{\mathrm{th}}$, as follows.

if $\overline{\sigma_{\mathrm{ASG}}^{(m)}} < \sigma_{\mathrm{ASG}}^{\mathrm{th}}$, grouping operation proceeds to the next stage;

$$m \leftarrow m + 1. \tag{22}$$

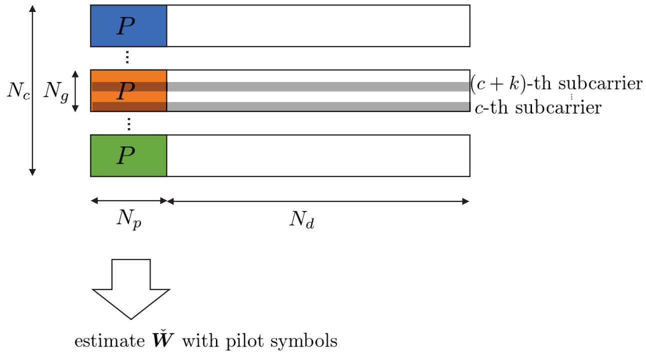

Fig. 2. Initial weight $\check{W}$ calculation with subcarrier grouping.

Otherwise, if $\overline{\sigma_{\mathrm{ASG}}^{(m)}} > \sigma_{\mathrm{ASG}}^{\mathrm{th}}$, the grouping process is terminated, and the array weight is calculated;

$$\hat{\boldsymbol{X}}_{c+k} = \overline{\boldsymbol{X}^{(m)}}, \tag{23}$$
$$\hat{\boldsymbol{P}}_{c+k} = \overline{\boldsymbol{P}^{(m)}}, \tag{24}$$
$$\boldsymbol{\Phi}_{\mathrm{SG}}^{c+k} = \hat{\boldsymbol{X}}_{c+k} \hat{\boldsymbol{X}}_{c+k}^{\mathsf{H}}, \tag{25}$$
$$\hat{\boldsymbol{V}}_{c+k} = \hat{\boldsymbol{X}}_{c+k} \hat{\boldsymbol{P}}_{c+k}^{\mathsf{H}}, \tag{26}$$
$$\hat{\boldsymbol{W}}_{c+k} = (\boldsymbol{\Phi}_{\mathrm{SG}}^{c+k})^{-1} \hat{\boldsymbol{V}}_{c+k}, \tag{27}$$

where $\hat{\boldsymbol{X}}_{c+k} \in \mathbb{C}^{N_\mathrm{r} \times N_\mathrm{P}}, \hat{\boldsymbol{P}}_{c+k} \in \mathbb{C}^{N_\mathrm{u} \times N_\mathrm{P}}, \boldsymbol{\Phi}_{\mathrm{ASG}}^{c+k} \in \mathbb{C}^{N_\mathrm{r} \times N_\mathrm{r}}, \hat{\boldsymbol{V}}_{c+k} \in \mathbb{C}^{N_\mathrm{r} \times N_\mathrm{u}}, \hat{\boldsymbol{W}}_{c+k} \in \mathbb{C}^{N_\mathrm{r} \times N_\mathrm{u}}$ denote the averaged received signal for grouping, the pilot signal matrix for grouping, the covariance matrix, CSI, and the proposed weight matrix at the $(c+k)$-th subcarrier $(k = 0, \ldots, m)$, respectively. Therefore, the optimal group size can be obtained. If $\sigma_{\mathrm{ASG}}^{\mathrm{th}}$ is set to an appropriate value, the ability to mitigate noise can be enhanced, contributing to better weight derivation.

III. Proposal: Subcarrier Grouping with Data-Aided Weight

In the adaptive subcarrier grouping, since setting a threshold too large degrades weight derivation accuracy due to an excess of data symbols having uncorrelated frequency characteristics, setting the appropriate value of $\sigma_{\mathrm{ASG}}^{\mathrm{th}}$ holds a prominent factor. SNR is considered to be the main factor involved in setting the threshold. Therefore, SNR estimation needs to be applied, such as some comparisons and novel algorithms [16]- [17]. However, if these algorithms are applied, it will increase the complexity of communication. [15] does not consider the computational problem and estimation accuracy. In the proposed method, we not only reduce the noise effect by increasing the number of data-aided samplings but also reduce the computational complexity while ensuring transmission efficiency. At this time, we do not use the additional pilot symbols. Our method is divided into two steps: 1. Deriving decision result of array output by the SMI with subcarrier grouping, 2. Obtaining a more accurate CSI vector aided by feedback decision data and estimating weight by LMS scheme with subcarrier grouping.

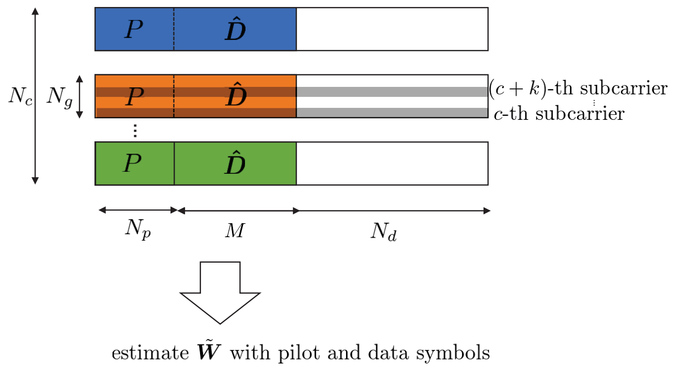

Fig. 3. Proposed weight $\tilde{W}$ calculation with subcarrier grouping.

Algorithm 1 Proposed interference suppression scheme

$\check{\boldsymbol{W}}_{c+k} \leftarrow (\boldsymbol{\Phi}_{\mathrm{SG}}^{c+k})^{-1}\hat{\boldsymbol{V}}_{c+k}$
$\boldsymbol{Y}_c \leftarrow \check{\boldsymbol{W}}_c^{\mathsf{H}}\boldsymbol{S}_c$
$\hat{\boldsymbol{D}}_c \leftarrow \mathcal{F}(\boldsymbol{Y}_c)$
$\tilde{\boldsymbol{D}}_c = [\boldsymbol{P}_c, \hat{\boldsymbol{D}}_c]$
$\overline{\boldsymbol{D}} \leftarrow \frac{1}{N_g}\sum_{k=0}^{N_g-1}\tilde{\boldsymbol{D}}_{c+k}$
$n \leftarrow 1$
$\tilde{\boldsymbol{W}}_{c+k}(n) \leftarrow \check{\boldsymbol{W}}_{c+k}$
while $n > L$ **do**
  $\tilde{\boldsymbol{W}}_{c+k}(n+1) \leftarrow$lms$[\tilde{\boldsymbol{W}}_{c+k}(n), \overline{\boldsymbol{D}}]$
  $n \leftarrow n+1$
end while
*lms[.] denotes the least mean square function

A. Initial Weight Calculation

Initial weight is calculated by SMI weight, which uses subcarrier grouping. Different from ASG, the grouping is not established according to the threshold. Each group is directly composed of the same number of subcarriers and the number of subcarriers is N_g. The initial weight $\check{\boldsymbol{W}}_{c+k}$ $(k = 0, \dots, N_g - 1)$ is calculated from (23) to (27). The range of the group from the $c-$th subcarrier is directly delimited as follows, without iteration,

$$m + 1 = N_g. \tag{28}$$

The array output for the c-th subcarrier is written by,

$$\boldsymbol{Y}_c = \check{\boldsymbol{W}}_c^{\mathsf{H}}\boldsymbol{S}_c. \tag{29}$$

Due to the noise effect, the initial array output contains the errors. It is mapped into the original QAM constellation points and the initial solution $\hat{\boldsymbol{D}}_{\boldsymbol{c}}$ is obtained as follows,

$$\hat{\boldsymbol{D}}_c = \mathcal{F}(\boldsymbol{Y}_c), \tag{30}$$

where $\mathcal{F}(.)$ represents the decision function. In order to reduce the amount of calculation, $\hat{\boldsymbol{D}}_c$ is only determined by the $M(0 \leq M \leq N_d)$ symbols instead of all. The concept of initial weight estimation for the SMI with subcarrier grouping is shown in fig. 2. Each group corresponding to a different color contains N_g subcarriers.

B. Data-aided Weight Calculation

In the data-aided weight calculation scheme, the subcarrier grouping is also used and $\hat{\boldsymbol{D}}_c$ can be regarded as an additional pilot signal for weight calculation and combined with the pilot signal as follows,

$$\tilde{\boldsymbol{D}}_c = [\boldsymbol{P}_c, \hat{\boldsymbol{D}}_c], \tag{31}$$

where $\tilde{\boldsymbol{D}}_c$ is desired response. The desired response in the subcarrier grouping can be derived as,

$$\overline{\boldsymbol{D}} = \frac{1}{N_g}\sum_{k=0}^{N_g-1}\tilde{\boldsymbol{D}}_{c+k}. \tag{32}$$

where the number of subcarrier grouping for the desired responses is N_g, similar to (19) and (28). Because of the inverse matrix operation, the repeated use of the SMI method results in a significant increase in computation. Therefore, we use the initial weight $\check{\boldsymbol{W}}_c$ and the LMS method to replace SMI.

$$\tilde{\boldsymbol{W}}_{c+k}(1) = \check{\boldsymbol{W}}_{c+k}, \tag{33}$$

$$\tilde{\boldsymbol{W}}_{c+k}(n+1) = \tilde{\boldsymbol{W}}_{c+k}(n) + \beta\tilde{\boldsymbol{X}}_{c+k}(\overline{\boldsymbol{D}}^{\mathsf{H}} - \tilde{\boldsymbol{X}}_{c+k}^{\mathsf{H}}\tilde{\boldsymbol{W}}_{c+k}(n)), \tag{34}$$

where n and β denote the number of iterations and the step size that can control the convergence characteristics of the LMS algorithm, respectively. $\tilde{\boldsymbol{W}}_{c+k}(n) \in \mathbb{C}^{N_{\mathrm{r}} \times N_{\mathrm{u}}}$ represents the weight at the $(c+k)$-th subcarrier in the n-th step of the LMS algorithm $(k = 0, \dots, N_g - 1)$. $\tilde{\boldsymbol{X}}_{c+k} \in \mathbb{C}^{N_{\mathrm{r}} \times (N_{\mathrm{p}}+M)}$ indicates the signal containing the X_c and the first M data symbols of the S_c with grouping and averaging. Grouping and averaging are performed as (23). In addition, since the initial state of the weight is calculated by the SMI algorithm, the number of iterations required for convergence can be decreased. Consequently, the amount of computation is reduced. It is worth noting that since the convergence rate of LMS without the initial weight is slower than SMI [22] [23], a large number of iterations must be performed to achieve the same satisfactory convergence as SMI. In other words, LMS without the initial weight is more computationally intensive than SMI in order to achieve the same effect. That is why the LMS cannot be used in the initial weight calculation. By repeating the above procedures, the weight error can be minimized. The concept of data-aided weight derivation for the LMS with subcarrier grouping is shown in Fig. 3. Algorithm 1 summarizes the detailed procedure (28)-(34).

IV. Computer Simulation

A. Simulation Parameters

We examine the interference suppression performance of the proposed algorithm by a computer simulation. Detailed simulation parameters are listed in Table I. The receiver using $N_{\mathrm{r}} = 16$ rectangular array antenna elements attempts to separate out one desired signal from $N_{\mathrm{u}} = 4$ incoming signals.

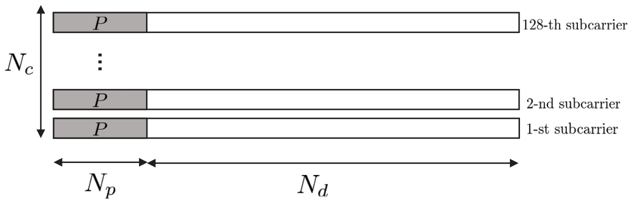

Fig. 4. Frame structure.

TABLE I
SIMULATION PARAMETERS

Parameters	Values
Number of receiver antennas N_{r}	16
Number of signal sources N_{u}	4
Transmission scheme	OFDM
Subcarrier spacing	15 kHz
Symbol duration T_{s}	71.4 μs
Modulation order	16QAM (w/o FEC)
Number of pilot symbols N_{p}	4
Number of data symbols N_{d}	30
Number of subcarriers N_{c}	128
Number of FFT points N_{FFT}	128
Angle of desired signal	$0°$
Angles of interference signals	$30°$, $-70°$, $80°$
Channel model	Rician fading
Rician K factor	10,-10 dB
Max Doppler frequency f_{d}	10 Hz ($f_{\mathrm{d}}T_{\mathrm{s}} = 4.0\times10^{-5}$)

We employ 16QAM modulation to every frame consisting of $N_{\mathrm{p}} = 4$ pilot and $N_{\mathrm{d}} = 30$ data symbols, and each frame is shown in Fig. 4. Moreover, each OFDM symbol is composed of $N_{\mathrm{c}} = 128$ subcarriers. Rician fading with multipath is considered. The bandwidth of the transmission signal is 1.25 MHz, and the OFDM symbol duration is $T_{\mathrm{s}} = 71.4$ μs, then the OFDM symbol rate is about $1/T_{\mathrm{s}} = 14$ kHz. These parameters are almost compatible with a compact cellular system, i.e. LTE system [24].

B. Simulation Results

Figs. 5 and 6 show the BER performance comparison between the conventional SMI, CCM-SMI, adaptive subcarrier grouping [15], and the proposed method. The effect of the conventional and proposed methods is evaluated with different LOS components. Rician K factors, i.e. $K = 10, -10$ dB, present whether the LOS component dominates the channel. When $K = -10$ dB, it approximates Rayleigh fading with no dominant LOS path. In the adaptive subcarrier grouping method, the value of σ_{ASG} according to the SNR and shown as follows,

$$\sigma_{\mathrm{ASG}} = \sqrt{\frac{10^{-3/10}}{SNR}}, \tag{35}$$

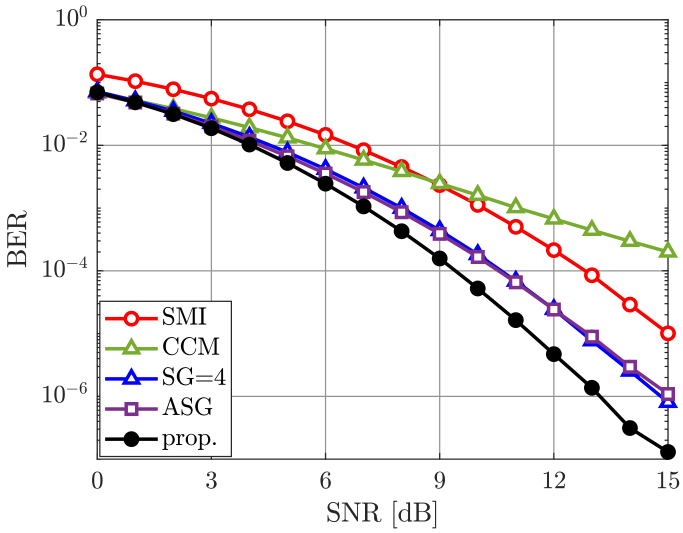

Fig. 5. BER performance comparison ($K = 10$ dB).

To achieve convergence while reducing the computational complexity, we set $M = 15$, $\beta = 0.6$, $L = 2$, $N_g = 4$ in the proposed method.

The proposed method has better BER performance than other conventional methods at arbitrary K factors. In a large $K = 10$ dB factor, the achievable gain is around 1.5 dB compared to ASG, and 4 dB compared to MMSE-SMI at 10^{-4} BER. Furthermore, in a smaller $K = -10$ dB situation, the proposed method also shows the best BER performance, where the achievable gain is around 1 dB compared to MMSE-SMI. However, although CCM-SMI can suppress the noise effect, the BER performance seriously deteriorates and the error floor is observed before 10^{-4} or 10^{-2} because of frequency selectivity. Therefore, it can only be used in a single-path situation. In addition, it is worth noting that ASG needs know the SNR situation to determine the threshold σ_{ASG} and make groups for noise rejection. In Figs. 5 and 6, the SNR estimation of ASG is assumed to be absolutely correct without considering the accuracy. If the performance of the SNR estimation method deteriorates, ASG will become ineffective. In addition, the proposed method does not depend on the SNR. It uses the same number of subcarrier groupings and decision feedback to improve BER performance.

C. Computation Complexity

Since a large number of weight calculations require huge memory and hardware resources, it is crucial to minimize the amount of computation with maintaining good performance. The number of complex-valued multiplications is used to evaluate the amount of computation.

Compared with the SMI algorithm, the computation complexity of our proposed scheme can be reduced by 20.4%. It is worth noting that although the decision feedback causes an increase in the amount of computation, several subcarriers can share one weight in the subcarrier grouping and the LMS algorithm is applied, which reduces the amount of computation. The LMS algorithm reuses the weight from the initial

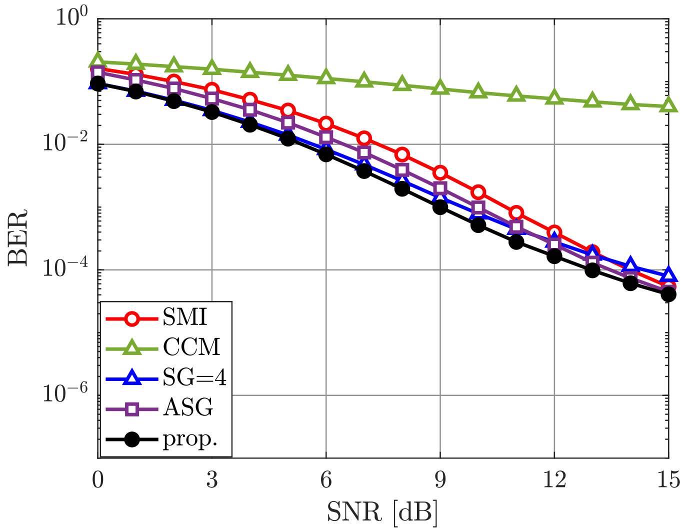

Fig. 6. BER performance comparison ($K = -10$ dB).

TABLE II
COMPUTATION COMPLEXITY

Algorithms	Values (example values used in simulation)
SMI per subcarrier	$N_{\mathrm{r}}^2 N_{\mathrm{p}} N_{\mathrm{c}} + N_{\mathrm{p}} N_{\mathrm{r}} N_{\mathrm{u}} N_{\mathrm{c}} + N_{\mathrm{r}}^3 N_{\mathrm{c}} + N_{\mathrm{r}}^2 N_{\mathrm{u}} N_{\mathrm{c}}$ (819,200)
Proposed	$(\mathrm{SMI} + 2\mathrm{L}\mathrm{N_c}\mathrm{N_u}(\mathrm{N_p} + \mathrm{M})\mathrm{N_r})\frac{1}{\mathrm{N_g}} + \mathrm{N_r}\mathrm{M}\mathrm{N_c}\mathrm{N_u} +$ $N_{\mathrm{c}} M N_{\mathrm{u}} \log_2(M N_{\mathrm{u}})$ (651,572)

phase as well as replaces matrix inversion that dominates the computational complexity.

V. CONCLUSION

This paper proposed the data-aided weight calculation and LMS method to improve the interference suppression performance of subcarrier grouping-based SMI adaptive array without SNR estimation method. It focuses on increasing data samples to reduce noise, thus maximizing the array weight derivation precision. Simulation results showed that the proposed method attained improved BER performance significantly with maintaining the transmission efficiency, whether LOS is the major factor or not. In addition, it saves computation compared to the conventional calculation of weight derivation for each subcarrier individually. Therefore, our proposed method can be applied as a potential future interference suppression technique for 5G or beyond, where small cells are heterogeneously deployed on the macro cells.

ACKNOWLEDGEMENT

This study was funded in part by a Grant of Scientific Research No. 22K04085 from the Japan Society for the Promotion of Science (JSPS), the Public Foundation of Chubu Science and Technology Center, and the Murata Science Foundation.

REFERENCES

[1] X. Chen, D. W. K. Ng, W. Yu, E. G. Larsson, N. Al-Dhahir and R. Schober, “Massive Access for 5G and Beyond,” *IEEE Journal on Selected Areas in Communications*, vol. 39, no. 3, pp. 615-637, Mar. 2021. DOI: 10.1109/JSAC.2020.3019724.

[2] K. Shafique, B. A. Khawaja, F. Sabir, S. Qazi and M. Mustaqim, “Internet of Things (IoT) for Next-Generation Smart Systems: A Review of Current Challenges, Future Trends and Prospects for Emerging 5G-IoT Scenarios,” *IEEE Access*, vol. 8, pp. 23022-23040, 2020, doi: 10.1109/ACCESS.2020.2970118.

[3] X. Wang et al., “Millimeter Wave Communication: A Comprehensive Survey,” *IEEE Communications Surveys and Tutorials*, vol. 20, no. 3, pp. 1616-1653, thirdquarter 2018. DOI: 10.1109/COMST.2018.2844322.

[4] Z. Pi and F. Khan, “An introduction to millimeter-wave mobile broadband systems,” *IEEE Communications Magazine*, vol. 49, no. 6, pp. 101-107, Jun. 2011. DOI: 10.1109/MCOM.2011.5783993.

[5] E. Björnson, M. Kountouris and M. Debbah, “Massive MIMO and small cells: Improving energy efficiency by optimal soft-cell coordination,” *ICT 2013*, 2013, pp. 1-5. DOI: 10.1109/ICTEL.2013.6632074.

[6] W. Saad, M. Bennis and M. Chen, “A Vision of 6G Wireless Systems: Applications, Trends, Technologies, and Open Research Problems,” *IEEE Network*, vol. 34, no. 3, pp. 134-142, May/June 2020. DOI: 10.1109/MCOM.2011.5783993.

[7] T. M. Duong and S. Kwon, “Vertical Handover Analysis for Randomly Deployed Small Cells in Heterogeneous Networks,” *IEEE Transactions on Wireless Communications*, vol. 19, no. 4, pp. 2282-2292, April 2020. DOI: 10.1109/TWC.2019.2963829.

[8] G. Giunta, C. Hao, and D. Orlando, “Estimation of rician K-factor in the presence of Nakagami-m shadowing for the LOS component,” *IEEE Wireless Commun. Lett.*, vol. 7, no. 4, pp. 550-553, Aug. 2018. DOI: 10.1109/LWC.2018.2794447

[9] Y. Hara, “Weight-convergence analysis of adaptive antenna arrays based on SMI algorithm,” *IEEE transactions on wireless communications*, vol. 2, no. 4, pp. 749-757, 2003. DOI: 10.1109/TWC.2003.814333

[10] S. Mubeen, A. M. Prasad and A. J. Rani, “Smart antennas by using LMS and SMI algorithms reduces interfernce,” *2016 International Conference on Electrical, Electronics, and Optimization Techniques (ICEEOT)*, pp. 204-208, 2016. DOI: 10.1109/ICEEOT.2016.7755027.

[11] X. Yuan and L. Gan, “Robust adaptive beamforming via a novel subspace method for interference covariance matrix reconstruction,” *Signal Processing*, vol. 130, pp. 233-242, 2017. DOI: 10.1016/j.sigpro.2016.07.008.

[12] T. Akao, S. Taroda, K. Maruta and C. -J. Ahn, “Improved common correlation matrix based SMI algorithm by channel estimation error minimization with LMS approach,” *2017 20th International Symposium on Wireless Personal Multimedia Communications (WPMC)*, pp. 63-67, 2017. DOI: 10.1109/WPMC.2017.8301888.

[13] C. -J. Ahn, and S. Iwao, “Adaptive array antenna based on radial basis function network as multiuser detection for WCDMA,” *Electronics Letters*, vol. 38, no. 20, pp. 1208-1210, 2002. DOI: 10.1049/el:20020756.

[14] K. Shima, K. Maruta and C. -J. Ahn, ”Data-aided SMI algorithm using common correlation matrix for adaptive array interference suppression,” *IEICE Transactions on Fundamentals of Electronics, Communications and Computer Sciences*, vol. 104, no. 2, pp. 404-411, 2021. DOI: https://doi.org/10.1587/transfun.2020SDP0001

[15] K. Shima, S. Kojima, K. Ito, K. Maruta and C. -J. Ahn, “Adaptive Subcarrier Grouping for MMSE-SMI Adaptive Array Interference Suppression,” *IEEE Access*, vol.9, pp. 18361-18372, 2021. DOI: 10.1109/ACCESS.2021.3053989

[16] S. Kojima, K. Maruta, Y. Feng, C. -J. Ahn and V. Tarokh, “CNN based Joint SNR and Doppler Shift Classification using Spectrogram Images for Adaptive Modulation and Coding,” *IEEE Transactions on Communications*, vol. 69, no. 8, pp. 5152-5167, Aug. 2021. DOI: 10.1109/TCOMM.2021.3077565.

[17] T. Ngo, B. Kelley and P. Rad, “Deep Learning Based Prediction of Signal-to-Noise Ratio (SNR) for LTE and 5G Systems,” *2020 8th International Conference on Wireless Networks and Mobile Communications (WINCOM)*, pp. 1-6, 2020. DOI: 10.1109/WINCOM50532.2020.9272470

[18] J. Tian, T. Zhou, T. Xu, H. Hu and M. Li, “Blind Estimation of Channel Order and SNR for OFDM Systems,” *IEEE Access*, vol. 6, pp. 12656-12664, 2018, doi: 10.1109/ACCESS.2017.2788020.

[19] T. Ngo, B. Kelley and P. Rad, “SNR estimation based on CNN and LSTM in broadcasting channel,” *2022 IEEE International Symposium on Broadband Multimedia Systems and Broadcasting (BMSB)*, pp. 1-6, 2022. DOI: 10.1109/BMSB55706.2022.9828573.

[20] N. Czink, X. Yin, H. OZcelik, M. Herdin, E. Bonek and B. H. Fleury, "Cluster Characteristics in a MIMO Indoor Propagation Environment," *IEEE Transactions on Wireless Communications*, vol. 6, no. 4, pp. 1465-1475, Apr. 2007. DOI: 10.1109/TWC.2007.348343

[21] Andreas F. Molisch, "Statistical Description of the Wireless Channel," *Wireless Communications*, IEEE, pp.69-99, 2011. DOI: 10.1002/9781119992806.ch5

[22] M. Al-Sadoon, R .A. Abd-Alhameed, I. T. E. Elfergani, J. M. Noras, J. Rodriguez, S. M. R. Jones, "Weight Optimization for Adaptive Antenna Arrays Using LMS and SMI Algorithms," *WSEAS Transactions on Communications*, vol. 15, pp. 206-214, 2016.

[23] B. S. Basha, and M. M. Ismail, "Study and Analysis of Beamforming Algorithm between LMS and SMI," *Journal of Communications*, vol. 17, no. 6, pp. 472-477, Jun 2022.

[24] M. H. Alsharif, R. Nordin, M. M. Shakir and A. M. Ramly, "Small cells integration with the macro-cell under LTE cellular networks and potential extension for 5G," *Journal of Electrical Engineering and Technology*, vol. 14, no. 6, pp. 2455-2465, 2019. DOI: 10.1007/s42835-019-00173-2

He He received the B.E. in Electrical and Electronics Engineering from Dalian Maritime University, Dalian, China, in 2018 and the M.E. degree in Electrical and Electronics Engineering from Chiba University, Chiba, Japan in 2020. He is now doing his Ph.D. program in the Chiba University. His research interests include machine learning and development of next generation communication algorithm. He received the IEEE VTS Tokyo/Japan Chapter 2021 Young Researcher's Encouragement Award, in 2021.

Jun-Han Wang received the B.E., M.E. degrees in electrical information engineering and machine learning from Dalian Maritime University, China, and Hiroshima University, Japan, in 2018 and 2022, respectively. He is currently pursuing a Ph.D. in Communication Systems and Machine Learning at Chiba University, Japan. He is currently working on channel estimation in high-speed environments using NLP methods.

Shun Kojima received the B.E., M.E., and Ph.D. degrees in electrical and electronics engineering from Chiba University, Japan, in 2017, 2018, and 2021, respectively. He is currently an Assistant Professor at the Graduate School of Engineering, Utsunomiya University. His research interests include machine learning, wireless communications, and signal processing. He is a member of IEICE. He received the Soft- COM Best Paper Award, in 2018, the 3rd Communication Quality StudentWorkshop Best Poster Award, in 2019, the IEEE VTS Tokyo/Japan Chapter 2020 Young Researcher's Encouragement Award, in 2020, the RISP Best Paper Award, in 2021, and the IEICE Radio Communication Systems Active Researcher Award, in 2021.

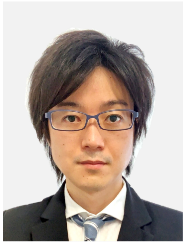

Kazuki Maruta received the B.E., M.E., and Ph.D. degrees in engineering from Kyushu University, Japan in 2006, 2008 and 2016, respectively. From 2008 to 2017, he was with NTT Access Network Service Systems Laboratories and was engaged in the research and development of interference compensation techniques for future wireless communication systems. From 2017 to 2020, he was an Assistant Professor in the Graduate School of Engineering, Chiba University. From 2020 to 2022, He was a Specially Appointed Associate Professor in the Academy for Super Smart Society, Tokyo Institute of Technology. He is currently an Associate Professor with Faculty of Engineering, Tokyo University of Science. His research interests include MIMO, adaptive array signal processing, channel estimation, medium access control protocols and moving networks. is a member of the IEEE and The Institute of Electronics, Information and Communication Engineers (IEICE). He received the IEICE Young Researcher's Award in 2012, the IEICE Radio Communication Systems (RCS) Active Researcher Award in 2014, APMC2014 Prize, and the IEICE RCS Outstanding Researcher Award in 2018. He was a co-recipient of the IEICE Best Paper Award in 2018, SoftCOM2018 Best Paper Award and APCC2019 Best Paper Award.

Chang-Jun Ahn received the Ph.D. degree in the Department of Information and Computer Science from Keio University, Japan in 2003. From 2001 to 2003, he was a research associate in the Department of Information and Computer Science, Keio University. From 2003 to 2006, he was with the Communication Research Laboratory, Independent Administrative Institution (now the National Institute of Information and Communications Technology). In 2006, he was on assignment at ATR Wave Engineering Laboratories. In 2007, he was with the Faculty of Information Sciences, Hiroshima City University as a lecturer. Now, he is working at the Graduate School of Engineering, Chiba University as a professor. His research interests include OFDM, digital communication, channel coding, and signal processing for telecommunications. He served as an associate editor of the IEICE Trans. on Fundamentals. From 2005 to 2006, he was an expert committee member for emergence communication committee, Shikoku Bureau of Telecommunications, Ministry of Internal Affairs and Communications (MIC), Japan. Dr. Ahn received the ICF research grant award for Young Engineer in 2002, the Funai Information Science Award for Young Scientist in 2003, the Distinguished Service Award from Hiroshima City in 2010, IEEE SoftCOM2018 Best Paper Award in 2018, IEEE APCC2019 Best Paper Award in 2019, IEICE ICETC2020 Best Paper Award in 2020, and Journal of Signal Processing Best Paper Award in 2021. He is a senior member of IEICE and IEEE.